

## Article

# Curcumin and quercetin loaded nanoemulsion: physicochemical compatibility study and validation of a simultaneous quantification method

**Gustavo Vaz** <sup>1,2</sup>, **Adryana Clementino** <sup>3</sup>, **Juliana Bidone** <sup>4</sup>, **Marcos Villetti** <sup>5</sup>, **Mariana Falkembach** <sup>1</sup>, **Matheus Batista** <sup>1</sup>, **Paula Barros** <sup>1</sup>, **Cristiana Dora** <sup>1,\*</sup> and **Fabio Sonvico** <sup>3,\*</sup>

<sup>1</sup> Laboratório de Nanotecnologia Aplicada à Saúde, Programa de Pós-Graduação em Ciências da Saúde, Universidade Federal do Rio Grande, Rio Grande (RS) Brazil; [mari\\_falkembach@hotmail.com](mailto:mari_falkembach@hotmail.com) (M.F.); [mbmatheus54@gmail.com](mailto:mbmatheus54@gmail.com) (M.B.); [alicebarros.pb@gmail.com](mailto:alicebarros.pb@gmail.com) (P.B.); [cristianadora@gmail.com](mailto:cristianadora@gmail.com) (C.D.)

<sup>2</sup> Coordenação de Aperfeiçoamento de Pessoal de Nível Superior – Brazil (CAPES); [richtervaz@gmail.com](mailto:richtervaz@gmail.com) (R.V.)

<sup>3</sup> Food and Drug Department, University of Parma, Parma (PR) Italy; [adryanarc@gmail.com](mailto:adryanarc@gmail.com) (A.C.); [fabio.sonvico@unipr.it](mailto:fabio.sonvico@unipr.it) (F.S.)

<sup>4</sup> Centro de Ciências Químicas, Farmacêuticas e de Alimentos, Universidade Federal de Pelotas, Pelotas (RS) Brazil; [julianabidone@gmail.com](mailto:julianabidone@gmail.com) (J.B.)

<sup>5</sup> Laboratório de Espectroscopia e Polímeros, Departamento de Física, Universidade Federal de Santa Maria, Santa Maria (RS) Brasil; [mvilletti@hotmail.com](mailto:mvilletti@hotmail.com) (M.V.)

\* Correspondence: [fabio.sonvico@unipr.it](mailto:fabio.sonvico@unipr.it) Telephone: +39 0521 906282 (F.S.); [cristianadora@gmail.com](mailto:cristianadora@gmail.com) Telephone: +55 53 32935313 (C.D.).

**Abstract:** Biphasic oily/water nanoemulsions have been proposed as delivery systems for the intranasal administration of curcumin (CUR) and quercetin (QU), due to their high drug entrapment efficiency, the possibility of simultaneous drug administration and protection of the encapsulated compounds from the degradation. To better understand the physicochemical and biological performance of the selected formulation simultaneously co-encapsulating CUR and QU, a stability test of the compounds mixture was firstly carried out using X-ray powder diffraction and thermal analyses, such as differential scanning calorimetry (DSC) and thermogravimetric analyses (TGA). The determination and quantification of the encapsulated active compounds was then required being an essential tool for the development of innovative nanomedicines. Thus, a new HPLC–UV/Vis method for the simultaneous determination of CUR and QU in the nanoemulsions and their evaluation in stability studies in simulated biological fluids was developed and validated. The X-ray diffraction analyses demonstrated that no interaction between the mixture of active ingredients, if any, is strong enough to take place in the solid state. Moreover, the thermal analysis demonstrated that the CUR and QU are stable in the nanoemulsion production temperature range. The proposed analytical method for the simultaneous quantification of the two actives was selective and linear for both compounds in the range of 0.5 – 12.5 µg/mL ( $R^2 > 0.9997$ ), precise (RSD below 3%), robust and accurate (recovery  $100 \pm 5\%$ ). The method was validated in accordance with ICH Q2 R1 “Validation of Analytical Procedures” and CDER-FDA 2 validation of chromatographic methods” guideline. Furthermore, the low detection ( $LOD < 0.005 \mu\text{g/mL}$  for CUR and  $< 0.14 \mu\text{g/mL}$  for QU) and quantification limits ( $LOQ \leq 0.017 \mu\text{g/mL}$  for CUR and  $\leq 0.48 \mu\text{g/mL}$  for QU) of the method were suitable for the application to drug release and permeation studies planned for the development of the nanoemulsions. The method was then applied for the determination of nanoemulsions CUR and QU encapsulation efficiencies ( $> 99\%$ ), as well as for the stability studies of the two compounds in simulated biological fluids over time. The proposed method represents, to our knowledge, the only method for the simultaneous quantification of CUR, and QU in nanoemulsions.

**Keywords:** HPLC method, Curcumin, Quercetin, Thermal analysis, Nanoemulsion.



## 1. Introduction

Quercetin (QU) and curcumin (CUR) are natural compounds that present interesting properties for the therapy of several diseases. QU is a common flavonol found in many vegetables, berries, fruits, beverages, and nuts [1]. QU has been found to decrease the inflammatory state induced by cholesterol oxidation products, a risk factor in neurodegenerative diseases, to lower the expression of pro-inflammatory cytokines, such as interleukin-6, tumor necrosis factor- $\alpha$ , interleukin-1b, and to inhibit the expression/activity of the cyclooxygenase-2 (COX-2) by suppressing the COX-2 mRNA expression [2]. As a consequence, QU is considered able to prevent neural damage [3,4]. However, despite the absorption by passive diffusion of QU across the intestine, the overall bioavailability of this compound is low and significantly variable among individuals [5].

CUR is a hydrophobic polyphenol derived from the rhizome of *Curcuma longa* that present several medicinal properties similar to QU, such as anti-inflammatory, anti-oxidant, and anti-neurodegenerative effects [6,7]. Furthermore, it has been found to be able to slow down the progression of neuronal loss in adult male rats [8]. However, the most challenging drawbacks for its therapeutic use are the low water solubility, the low bioavailability, and the low blood concentrations after oral administration [9]. Taken together, the poor absorption from the gastrointestinal tract of CUR, its rapid metabolism in the liver and in the intestinal wall, and its limited blood brain barrier permeability are considered the main limitations to the therapeutic use of this compound in neurodegenerative disorders [10].

In fact, the role of oxidative stress and of the associated inflammation are becoming increasingly evident in the pathogenesis of neurodegenerative diseases [11–13]. The therapeutic potential of both CUR and QU is, however, further restricted by their poor stability in physiological environment. The use of innovative nanotechnology-based formulations has been proposed in many studies with the aim of improving the bioavailability of natural compounds similar to CUR and QU. Indeed, various nanocarrier systems have been demonstrated to provide interesting therapeutic benefits according on the nanocarrier properties, and the loaded pharmacologically active compound [14,15].

In this sense, the development of nanocarriers loaded with CUR and QU in combination (Figure 1) and able to protect and direct these substances to the brain could represent an interesting approach for the treatment of neurodegenerative diseases. The association of these compounds can be highly advantageous providing an alternative to current pharmacological treatments, since the two natural substances could act synergistically, and the use of these natural compounds could be economically advantageous in comparison to the development of new pharmacologically active chemical entities.

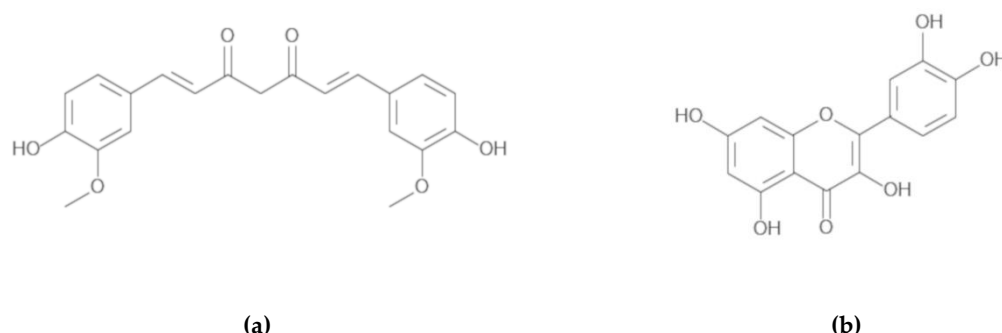


**Figure 1.** Chemical structures of curcumin (a) and quercetin (b).

Studies with nanoemulsions demonstrated that this type of nanocarriers can be a potential drug delivery systems for brain delivery [16]. These nanocarriers are kinetically stable and not significantly affected by creaming, coalescence, flocculation or sedimentation during storage time [17]. The formulations are generally non-toxic and non-irritant being manufactured using low concentrations of surfactants safe for human consumption (GRAS) [18]. Therefore, considering the lipophilicity of CUR and QU, nanoemulsions appear particularly advantageous for the formulation and delivery into

the brain of these natural compounds [19]. The large surface of the nanoemulsions enhance the permeation through biological barriers and in addition, the nanoemulsions can protect the encapsulated compounds from hydrolysis and oxidation. In fact, nanoemulsion-based formulations provide a number of significant and unique advantages favorable for drug delivery via a several administration routes [19].

Although advances in nanometric-sized formulations have opened the way to a new class of diagnostic and therapeutic nanomedicines for many diseases, their transfer from the benchtop research to currently marketed products are still limited. This lack of conversion is mostly attributed to problems with nanomedicines characterization, including physicochemical analyses, evaluation of their interaction with the biological environment and, often, the development of suitable analytical methods for encapsulated drug separation and determination. Chromatographic methods development and validation play important roles in the design, development and manufacture of nanosized pharmaceuticals due to their ability to separate and quantify several analytes of interest from the components of the nanocarriers. Indeed, the quantification of the pharmaceutically active compounds is required for the study of the nanosystems encapsulation efficiency, drug release kinetics, as well as stability and even for the investigation of their interaction with biological interfaces [20].

This paper reports the pre-formulation studies and analytical method validation for the development of a CUR/QU nanoemulsion, as the first step towards a new treatment of neurodegenerative disorders with the combination of these two compounds. In this sense, the development and characterization of this new pharmaceutical formulation required the evaluation of parameters such as drug content and stability of the nanoencapsulated compounds in comparison to free CUR and QU. Thus, in this work, a simple, sensitive, and specific high-pressure liquid chromatography (HPLC) method was developed and validated for the separation and simultaneous quantification of CUR and QU in a nanoemulsion. To evaluate the stability of CUR and QU, the validated analytical method was applied to monitor the content of the active ingredients during a stability study comparing the compound stability in a free and nanoencapsulated form.

## 2. Materials and Methods

### 2.1. Materials for analytical method development

Acetonitrile and methanol of HPLC grade used in the analysis were purchased from Panreac® (Barcelona, Spain). Ultrapure water was obtained from a Milli-Q water system (Millipore®, Burlington, MA, USA). Phosphoric acid (Reagen®, Rio de Janeiro, Brazil) used in the study was of analytical reagent grade.

### 2.2. Materials for nanoemulsion production and characterization

CUR, QU, PEG 660-stearate, and castor oil were purchased from Sigma-Aldrich (St. Louis, MO, USA). Egg lecithin (Lipoid E80®) and Purified Fish Oil (DHA/EPA) were purchased from Lipoid (Steinhausen, Switzerland). Polyethylene glycol 400 (PEG400) was purchased from Synth (São Paulo, Brazil). Ultrafree-MC® centrifugal filtration devices (10,000 Da MWCO) were purchased from Millipore® (Burlington, MA, USA). Uranyl acetate was purchased by Electron Microscopy Sciences (Hatfield, PA, USA) All other reagents, when not specified, were of analytical grade.

### 2.3. Compatibility study of curcumin and quercetin

#### 2.3.1. Preparation of curcumin/quercetin binary mixtures

The binary mixtures were prepared and mechanical homogenized with a mortar and pestle by taking CUR and QU in a 1:1 proportion by weight. These mixtures were further used for X-ray powder diffraction and thermal analyses.

#### 2.3.2. Thermal analyses

Thermogravimetric analysis (TGA) was performed using a TGA-50 equipment (Shimadzu, Kyoto, Japan) under a nitrogen atmosphere with a flow rate of 50 mL/min at a heating rate of 10 °C/min over the range from 0 to 900°C and using approximately 3 mg of sample in a platinum cell.

DSC data were collected on a DSC-60 instrument (Shimadzu, Kyoto, Japan). Approximately 1 mg samples were placed in aluminum pans, and the temperature ramp was set to increase from 50 to 225 °C with a heating rate of 10 °C/min under nitrogen flow (50 mL/min).

### 2.3.3. X-ray powder diffraction (PXRD)

PXRD patterns were collected on a D8 Advance instrument (Bruker, Billerica, MA, USA) operating at 1.5418 Å, 40 kV voltage, and a current of 40 mA using a Cu K- $\alpha$  radiation source. The samples were contained in a sample holder and the data acquisition was done in a 2  $\theta$  range from 2 to 70 degrees at 0.05 degrees every 2 seconds step size over a total period of 50 min.

### 2.3.4. Equipment and chromatographic conditions

Chromatographic analyses were performed on a Flexar HPLC system (Perkin Elmer Inc., Waltham, MA, USA) equipped with a quaternary pump, photodiode array detector, and automatic injection with a 15  $\mu$ L sample loop. The chromatographic separations were performed using a 150×4.6 mm i.d., 5  $\mu$ m particle size, C18 column (Zorbax ODS, Agilent Technologies, Wilmington, DE, USA) protected by a C18 guard column (150 $\mu$ m, 140Å, Phenomenex, Torrance, CA, USA) in gradient elution mode with a mobile phase obtained mixing aqueous phosphoric acid 1% w/v adjusted at pH 2.6 (Eluent A) and acetonitrile (Eluent B) at a flow rate of 1.0 mL/min (Table 1). The detection wavelength was set at 400 nm and oven temperature was maintained at 40±1°C during whole analysis time.

**Table 1.** Chromatographic conditions of the gradient HPLC analytical method

Time (min)	Eluent A (%)	Eluent B (%)	Flow rate (mL/min)
0.01	60	40	1.0
5.00	60	40	1.0
6.00	50	50	1.0
15.00	50	50	1.0

Eluent A: Phosphoric acid 1% w/v in water, pH 2.6; Eluent B: Acetonitrile

### 2.3.5. Preparation of stock and working solutions

Standard stock solutions of CUR and QU were freshly prepared by dissolving the compounds in methanol (1 mg/mL). Calibration curves were prepared using working solutions with concentration values 0.25, 0.5, 1.0, 2.5, 5.0, 7.5, 10.0 and 12.5  $\mu$ g/mL by diluting the stock solution in a standard diluent obtained by the binary mixture (50:50, v/v) of methanol and 1% phosphoric acid pH 2.6. An aliquot (15  $\mu$ L) of each working solution was then directly injected into the HPLC for further analysis.

### 2.3.6. HPLC method validation

The proposed HPLC method was validated under the optimized conditions regarding its linearity range, selectivity and system suitability, sensitivity, precision, accuracy, robustness, and stability of the assay according to the analytical methods validation requirements. The method was validated in accordance with ICH Q2 R1 (validation of Analytical Procedures: Text and Methodology) [21] and CDER-FDA guideline (validation of chromatographic methods) [22].

#### 2.3.6.1. Linearity range

The linearity range was evaluated by measuring the chromatographic peak area responses of the compounds at seven concentration levels and in triplicate. Calibration curves were constructed by plotting the peak area against the concentration of CUR and QU, which then were interpolated by linear regression.

#### 2.3.6.2. Selectivity and system suitability

To ensure the selectivity of the proposed method, a drug-free nanoemulsion was prepared and analyzed in the described chromatographic conditions. Subsequently, the chromatographic separation of the two analytes was evaluated using the highest work solution (12.5 µg/mL CUR/QU) to determine number of theoretical plates (N), analytes retention factor (K'), selectivity ( $\alpha$ ), symmetry (T), and to calculate peaks resolution (Rs) and area repeatability (calculated using the response relative standard deviation, RSD).

$$N = 5.55 \times \left( \frac{t_r}{W_h} \right)^2 \quad (1)$$

$$K' = \frac{t_r - t_0}{t_0} = \frac{t'_{rB}}{t_0} \quad (2)$$

$$\alpha = \frac{t'_{rB}}{t'_{rA}} = \frac{t_{rB} - t_0}{t_{rA} - t_0} = \frac{K'_{rB}}{K'_{rA}} \quad (3)$$

$$Rs = \frac{2 \cdot (t_{rA} - t_{rB})}{(W_b^A + W_b^B)} \quad (4)$$

Where:

$t_r$  = retention time

$t_0$  = dead time

$W_h$  = width at average peak height

$W_b$  = width at the base of the peak

#### 2.3.6.3. Sensitivity

The sensitivity was determined by means of the limit of detection (LOD) and limit of quantification (LOQ). One of the ways to calculate the LOD (Equation 5) and LOQ (Equation 6) is based on the standard deviation ( $\sigma$ ) of the y-intercepts and slope ( $s$ ) obtained from the equation obtained by linear regression of the calibration standards:

$$LOD = 3.3 \cdot \frac{\sigma}{s} \quad (5)$$

$$LOQ = 10 \cdot \frac{\sigma}{s} \quad (6)$$

#### 2.3.6.4. Precision and accuracy

The accuracy and precision of the method were estimated by sextuplicate quality control (QC) samples prepared using the standard diluent mixture (methanol:1% phosphoric acid pH 2.6) at the following concentrations 0.5 µg/mL (low QC), 2.5 µg/mL (medium QC), and 12.5 µg/mL (high QC) for both CUR and QU. Accuracy was established through back-calculation and expressed as the percent difference between the found and the nominal concentration for each compound, and the precision was calculated as the coefficient of variation (CV) of the replicate measurements. Calibration standards and QC samples were analyzed in three different batches in order to determine the intra and inter-batch variability. The intra-day precision (repeatability) was carried out by performing six consecutive analyses of standard solution at three different concentrations for each drug on the same day. The samples were also analyzed on different days to evaluate the inter-day

precision (repeatability). The obtained values were evaluated through the dispersion of the results by calculating the standard deviation of the measurement series.

#### 2.3.6.5. Robustness

The robustness of an analytical method is a measure of its capacity to resist changes due to small variations in parameter conditions. In this way, the method robustness was assessed as a function of changing the column temperature, mobile phase composition, and pH (Table 2). The time in which the variations of the mobile phase occurred were in accordance with the data in Table 1.

**Table 2.** Analytical parameters and their levels of changes used in the robustness test of the method for CUR and QU by HPLC.

Parameter	Condition
Column temperature	35°C
	40°C
	45°C
Mobile phase composition (aqueous phosphoric acid 1%:acetonitrile)	35:65/45:55
	40:60/50:50
	45:55/55:45
pH	2.3
	2.6
	2.9

#### 2.3.6.6. Stability

Two different evaluations were made to determinate compounds stability. Firstly the stability of the CUR and QU in solution (50:50, methanol:1% phosphoric acid, v/v; pH 2.6), was investigated after storage for 7, 15, and 30 days under refrigeration (8°C), and at room temperature (25°C) using a methanolic solution of 2.5 µg/mL of each compound as a control. In a second step, the comparison between the stability of the free CUR and QU and the nanoencapsulated compounds were evaluated during 4 hours in phosphate buffer (phosphate buffered saline, PBS pH 7.4:PEG 400 90:10 v/v) at 25°C and 37°C.

#### 2.3.7. Application of the method

##### 2.3.7.1. Nanoemulsion preparation

After the development of a simple, accurate and precise method, the nanoemulsion containing CUR and QU (CQ NE) was produced. Nanoemulsion was composed of egg lecithin, castor oil and purified fish oil (DHA/EPA), PEG 660-stearate and water. Nanoemulsion was formed via high-energy emulsification followed by high-pressure homogenization of a mixture of a water phase and an oil phase. To prepare the nanoemulsion loaded with CUR and QU, the oil and aqueous phases of the emulsion were firstly prepared separately. In order to prepare the water phase, the surfactant PEG 660-stearate was dissolved in ultrapure water (1.5% w/v). The oil phase containing castor oil, Lipoïd® Purified Fish Oil (DHA/EPA) and egg lecithin (Lipoïd E80®) was maintained for 30 min at 68°C under magnetic stirring at 1,500 rpm. The aqueous phase (60 mL) heated to 80 °C under magnetic stirring at 1,500 rpm for 2 minutes was then added to the oil phase. After adding the aqueous phase to the oil phase, the dispersion was homogenized for 2 minutes using a mechanic high performance dispersing device (Ultraturrax TP 18/10 – 10N; IKA-Werke GmbH, Staufen, Germany) at 14,500 rpm for 2 minutes to form the pre-emulsion. Finally, the pre-emulsion was processed with a high-pressure homogenizer (PandaPLUS 2000 Laboratory Homogenizer, GEA Niro Soavi, Parma, Italy), 13 cycles of 20 seconds each at 1,000 bar, totaling 4 minutes and 20 seconds. For the preparation of CQ NE, the CUR and QU compounds were added to the organic phase of the formulation and maintained under heating (68 °C) and stirring (1,500 rpm) for 30 minutes (Table 3).

**Table 3.** Composition of the nanoemulsion as prepared through the high pressure homogenization method

Formulation	PEG 660-stearate (%; w/v)*	Castor Oil (mg)	Purified fish oil (mg)	Egg lecithin (mg)	CUR (mg)	QU (mg)
CQ NE	1.5	2400	2400	1200	45	45
NE	1.5	2400	2400	1200	-	-

\* aqueous phase (60mL)

#### 2.3.7.2. Size and zeta potential measurements

The particle size and zeta potential of the NEs were determined by dynamic light scattering and laser doppler anemometry, respectively, using a Zetasizer Nano Series (Malvern Pananalytical, Malvern, UK). The particle size measurements were performed at 25 °C after appropriate dilution of the samples in distilled water (1:100). Each size analysis lasted 300 s and was performed with a detection angle of 90°. The hydrodynamic radius was determined according to Stokes- Einstein's equation (Equation 7):

$$R = \frac{\kappa B T}{6\pi\eta D} \quad (7)$$

Where:

$\kappa B$  = Boltzmann's constant (J/K)

T = temperature (in K)

D = diffusion coefficient

$\eta$  = viscosity of the medium–water in this case ( $\eta = 0.89$  cP at 25 °C)

For measurements of zeta potential, the samples were placed in the electrophoretic cell, where an alternating voltage of  $\pm 150$  mV was applied. The zeta potential values were calculated as mean electrophoretic mobility values using Smoluchowski's equation.

#### 2.3.7.3. Determination of curcumin and quercetin concentrations in the nanoemulsion

The CUR and QU content (total concentration) in the nanocarrier suspension was calculated after determining the drug concentration compared to the methanolic standard solution (2.5 µg/mL) and was expressed in mg/mL of CUR and QU. To perform the determination of the drug content the nanoemulsion was appropriately diluted (200 times) with methanol and phosphoric acid 1% (50:50, v/v; pH 2.6) for drugs extraction from the formulation matrix. The CUR and QU recovery was calculated as the percentage of the total drug concentration found in the nanocarrier suspension in relation to the initially added amount. The entrapment efficiency (%) was estimated indirectly as the difference between the total recovered amount of CUR and QU of the nanocarrier and that found in solution after eliminating the inner phase nanodroplets by ultrafiltration. The ultrafiltrate was obtained by an ultrafiltration/centrifugation method of an aliquot (500 µL) of the nanoemulsion using an Ultrafree-MC® (10,000 Da MWCO) Millipore® (Burlington, MA, USA) centrifugated at 10,000×g for 30 min (Sigma 3K30, Osterode am Harz, Germany). All samples were analyzed in triplicate.

### 2.3.7.4. Morphologic evaluation

The morphology of nanoemulsion was investigated using a Transmission Electron Microscope (TEM) (JEOL 1400, Indianapolis, IN, USA). A drop of the nanoemulsion was diluted suitably (1000 $\times$ ) with ultrapure water, deposited on a copper grid coated with carbon followed by addition of negative stain (20 $\mu$ L of uranyl acetate 2% w/v solution). After 20 min incubation at room temperature, excess liquid was carefully drained with a piece of filter paper and the samples were put into a desiccator overnight to completely eliminate the solvent. Images were captured using the TEM operated at 80 kV and 30,000 $\times$  magnification.

### 2.4. Data presentation and statistical analysis

Each experiment was conducted in triplicate, and the data are represented as mean and standard deviation. Statistical analysis was conducted using analysis of variance (ANOVA), followed by a *post-hoc* Bonferroni test; a p-value less than 0.05 ( $p < 0.05$ ) was considered statistically significant. All statistical analyses were performed using Prism software (ver. 8.4.3, Graph-Pad, San Diego, CA, USA).

## 3. Results

### 3.1. Pre-formulation studies with curcumin and quercetin

Thermogravimetric analyses of the two natural compounds and their mixture are presented in Figure 2. The TGA curves derivative (dTGA) (Figure 2b) shows that CUR was thermally stable up to 200 °C ( $T_{onset}$ ), when its thermal decomposition started. The decomposition ended at 427 °C. Concerning the mass loss, it was found that in this first step around 53% of the initial mass was lost. A second step of decomposition occurred in the range 428–900°C, with a further mass loss of 17%. The residual mass at 900°C was 30%.

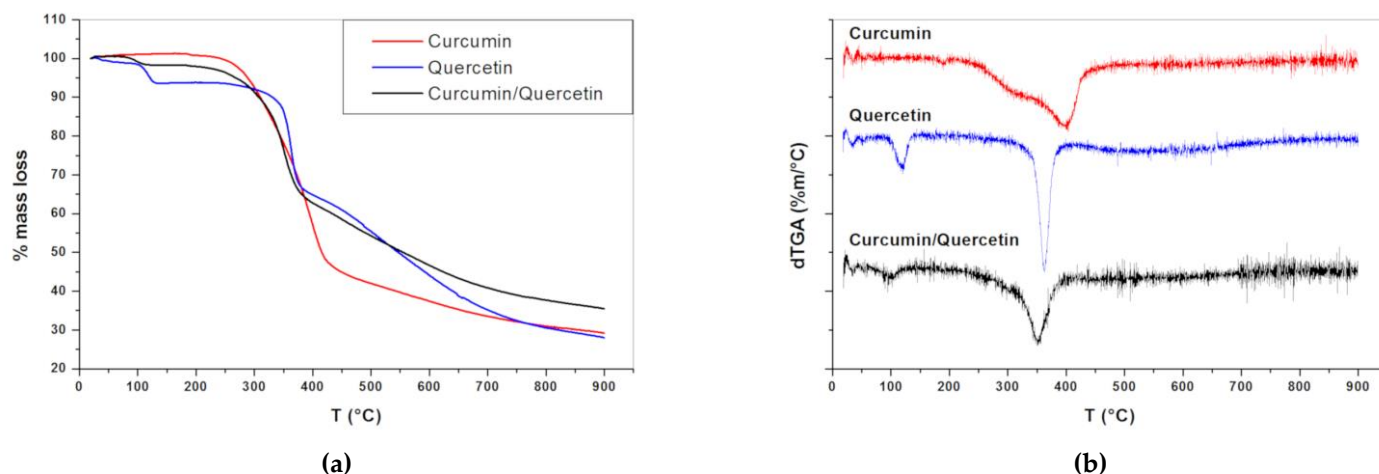


**Figure 2.** (a) Thermogravimetric analysis curves (TGA) and (b) first derivative of TGA curves (dTGA) obtained for curcumin, quercetin, and curcumin/quercetin binary mixture (1:1).

In the case of QU, a first mass loss (around 6.5%) occurred between 94 and 137 °C (Figure 2a and 2b) and could be attributed to the loss of water of the sample. In fact, the percentage of water loss observed was very similar to values reported in literature [23–25]. This result highlights that QU in the solid-state shows a certain degree of hydration of their crystal lattice, despite its lipophilicity. According to Borghetti and co-workers, quercetin hydrates occur due to the intermolecular hydrogen bonds between hydration water molecules and hydroxyl groups of the flavonoid [24]. In this way, the presence of water molecules into the crystal lattice of the QU influences its molecular geometry and crystalline structure, leading to great changes in its thermal stability, solubility, and bioavailability. A second mass loss step started at 240°C and ended at 385°C, with a mass loss of

27.3%. A third mass loss occurred in the range 386–900°C, with a mass loss of 38%. The residual mass at 900°C was 28.2%. The TGA profile of the binary physical mixture of CUR and QU (1:1 ratio) (Figure 2a and 2b) showed three decomposition steps. The first mass loss corresponded to the release of water molecules due to the presence of QU hydrates in the mixture, the percentage mass loss was lower when compared to pure QU and occurred in the range of 72 to 127 °C (Figure 2a and 2b). The second and third mass losses correspond to the thermal decomposition of the compounds (CUR and QU) at the highest temperatures, as observed for pure compounds. Overall, the TGA profile of the binary mixture did not suggest significant interactions in the solid-state between the two compounds. Similar results were obtained by DSC analysis.

The DSC curve for QU showed only one endothermic peak located in the range of 99 and 125 °C (maximum of the peak at 115°C) correspondent to the release of water from the crystal lattice. The temperature of the maximum of the peak was much higher than the boiling point of water which means that molecules of water are strongly held by the QU crystals through hydrogen bonding [25]. The melting point of QU was not observed (316°C) [26]. The CUR analysis showed only one endothermic peak in the range 172–183 °C (maximum of the peak at 176 °C), corresponding to the melting point of CUR reported in literature (175.1°C) [27]. Furthermore, a shoulder was observed in the DSC curve from 200 °C. Similar thermal events observed to pure compounds were detected in the DSC curve for binary mixture, meaning that non-significant interactions occur between CUR and QU in the solid-state (Figure 3a). Interestingly, powder X-ray diffraction (PXRD) analysis conducted on the same materials showed that the diffraction of the binary mixture (Figure 3b) contained all the peaks of CUR and QU, with no marked displacement of the peaks being observed, indicating a lack of interaction in the physical mixture of the two compounds.

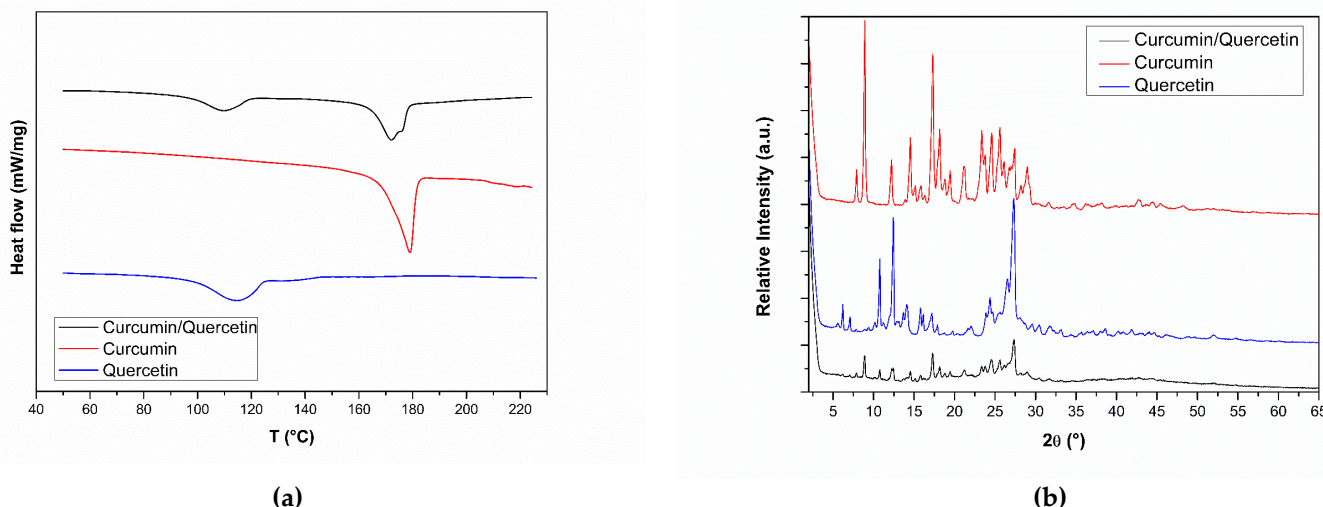


**Figure 3.** (a) Differential scanning calorimetry (DSC) profiles of curcumin, quercetin and the curcumin/quercetin binary mixture (1:1); (b) X-ray diffractograms of curcumin, quercetin and the curcumin/quercetin binary mixture (1:1).

### 3.2. Method development and validation

The best separation conditions for CUR and QU were achieved using a C18 analytical column in a gradient elution mode with a mobile phase composed of acetonitrile and an 1% phosphoric acid in water (Table 1), at a flow rate of 1.0 mL/min. The detection wavelength was set at 400 nm, and  $40 \pm 1^\circ\text{C}$ . A typical chromatogram is showed in Figure 4, with a retention time of 2.15 min being observed for QU, and 10.49 min for CUR. It was possible to observe three other peaks of non-interest in the chromatogram: an unidentified impurity (3.06 min) and the curcuminoids bisdemethoxycurcumin

(8.94 min) and demethoxycurcumin (9.71 min) [28]. However, none of them appear to interfere with the elution and separation of the investigated analytes.

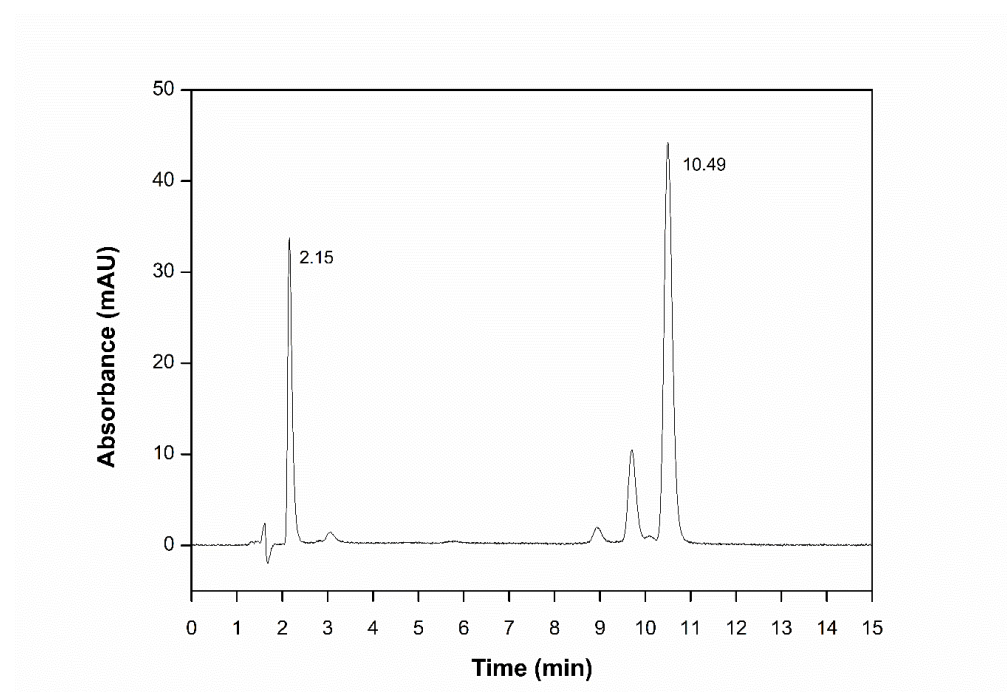


**Figure 4.** Chromatograms of the standard solution containing a binary mixture of curcumin and quercetin (12.5  $\mu$ g/mL).

To evaluate the linearity of the method, calibration standards of CUR (0.25–12.5  $\mu$ g/mL) and QU (0.25–12.5  $\mu$ g/mL) were analyzed. A linear relationship was established for the injected concentration ranges versus the peak area for both analytes, with determination coefficients greater than 0.9997. Some validation parameters obtained with the calibration standards are reported in Table 4, while the linearity parameters of the method shown in Table 5.

**Table 4.** Data related to the LOD, LOQ, slope, and interception for curcumin and quercetin HPLC analysis method.

	Parameters	Validation Results
Curcumin	Linearity	Calibration range ( $\mu$ g/mL): 0.5–12.5 $y = 40565x - 272.07$ ( $R^2=0.9998$ )
	LOD	0.005 $\mu$ g/mL
	LOQ	0.017 $\mu$ g/mL
	Slope	$40565 \pm 201$
Quercetin	Intercept	$-272.07 \pm 1246.54$
	Linearity	Calibration range ( $\mu$ g/mL): 0.5–12.5 $y = 18043x + 129.07$ ( $R^2=0.9997$ )
	LOD	0.14 $\mu$ g/mL
	LOQ	0.48 $\mu$ g/mL
	Slope	$18043 \pm 118$
	Intercept	$129.07 \pm 733.51$

**Table 5.** Data related to the linearity of the developed HPLC method with its respective average, precision, and accuracy.

Concentration ( $\mu\text{g/mL}$ )	Curcumin			Quercetin		
	Concentration found ( $\mu\text{g/mL}$ )	Accuracy (%)	Precision (%)	Concentration found ( $\mu\text{g/mL}$ )	Accuracy (%)	Precision (%)
0.5	0.497 $\pm$ 0.005	99.40 $\pm$ 1.10	1.20	0.518 $\pm$ 0.012	103.60 $\pm$ 2.54	2.69
1.0	1.024 $\pm$ 0.008	102.40 $\pm$ 0.85	0.87	1.008 $\pm$ 0.012	100.80 $\pm$ 1.85	2.08
2.5	2.503 $\pm$ 0.014	100.12 $\pm$ 0.56	0.59	2.501 $\pm$ 0.020	100.04 $\pm$ 0.88	0.87
5.0	5.005 $\pm$ 0.049	100.10 $\pm$ 0.98	0.99	4.993 $\pm$ 0.020	99.86 $\pm$ 0.40	0.40
7.5	7.517 $\pm$ 0.023	100.22 $\pm$ 0.30	0.30	7.489 $\pm$ 0.074	99.85 $\pm$ 0.99	1.10
10.0	10.019 $\pm$ 0.019	100.19 $\pm$ 0.19	0.20	9.982 $\pm$ 0.030	99.82 $\pm$ 0.30	0.34
12.5	12.579 $\pm$ 0.090	100.63 $\pm$ 0.76	0.86	12.496 $\pm$ 0.062	99.96 $\pm$ 0.49	0.53

The method's selectivity was confirmed by the absence of interferences at the retention times of CUR and QU in the chromatograms obtained when the nanoemulsion prepared without the drugs (data not shown).

The analytical method was suitable for the separation, detection and quantification of analytes, as shown on Table 6, with peaks presenting good shape (QU -  $K'$  0.47; CUR -  $K'$  6.18), symmetry (QU -  $T$  0.968; CUR -  $T$  0.909),  $\alpha$  13.14 and resolution  $Rs$  10.83. The system suitability of the developed method for QU and CUR showed a high value of resolution ( $Rs > 2$ , CDER-FDA acceptance criteria) [22], and the repeatability of peak area ( $RSD \leq 1\%$ ), as reported on Table 6. The intra- and inter-day precision relative standard deviation ( $RSD \%$ ) was between 0.8 and 5.9 for CUR and 0.4 and 7.6 for QU. The recovery of the drugs was in the range of 99.46–101.63% with RSDs below 4.2% for CUR and in the range of 93.60–103.73% with RSDs below 4.64% for QU. The results are presented in Table 7.

**Table 6.** System suitability chromatographic parameters

Analyte	N	K'	T	$\alpha$ (QU/CUR)	Rs (QU/CUR)
QU	3506	0.47	0.968	13.14	10.83
CUR	20774	6.18	0.909		

Abbreviations: N, number of theoretical plates;  $K'$ , retention factor; T, symmetry;  $\alpha$ , selectivity; Rs, resolution.

**Table 7.** Data related to the repeatability and intermediate precision of the developed HPLC method

Samples	Intra-Day Precision (Repeatability)				Inter-Day Precision (Repeatability)		
	Concentration ( $\mu\text{g/mL}$ )	Concentration found ( $\mu\text{g/mL}$ )	Accuracy (%)	Precision (%)	Concentration found ( $\mu\text{g/mL}$ )	Accuracy (%)	Precision (%)
Curcumin	0.5	0.50	101.63 $\pm$ 4.2	5.9	0.49	99.46 $\pm$ 1.10	1.2
	2.5	2.49	99.98 $\pm$ 1.0	1.5	2.50	100.12 $\pm$ 0.56	0.5
	12.5	12.65	101.26 $\pm$ 1.0	1.4	12.57	100.63 $\pm$ 0.76	0.8
Quercetin	Concentration ( $\mu\text{g/mL}$ )	Concentration found ( $\mu\text{g/mL}$ )	Accuracy (%)	Precision (%)	Concentration found ( $\mu\text{g/mL}$ )	Accuracy (%)	Precision (%)
	0.5	0.46	93.60 $\pm$ 4.64	7.6	0.51	103.73 $\pm$ 2.54	2.6

2.5	2.46	98.68 ± 1.84	3.2	2.50	100.06 ± 0.88	0.8
12.5	12.43	99.44 ± 0.67	1.1	12.49	99.97 ± 0.49	0.4

In order to evaluate the robustness of the chromatographic method, assays were carried out by analyzing standard solutions (2.5 µg/mL) under slight variations of the method conditions, including column temperature, mobile phase composition and pH. The results from the robustness testing are displayed in Table 8.

**Table 8.** Results obtained from the study of robustness of the HPLC method.

Variable	Value	Curcumin content <sup>a</sup> (µg/mL)	RSD <sup>a</sup> (%)	Quercetin content <sup>a</sup> (µg/mL)	RSD <sup>a</sup> (%)
Column temperature (°C)	35	2.53 ± 0.04	1.67	2.54 ± 0.02	0.82
	40	2.50 ± 0.03	1.59	2.50 ± 0.03	1.87
	45	2.51 ± 0.03	1.41	2.49 ± 0.01	0.40
Mobile phase composition (1% phosphoric acid:acetonitrile, v/v; pH 2.6)	35:65/45:55	2.51 ± 0.06	2.39	2.51 ± 0.06	2.58
	40:60/50:50	2.50 ± 0.03	1.59	2.50 ± 0.03	1.87
	45:55/55:45	2.51 ± 0.03	1.31	2.54 ± 0.05	2.09
pH of the mobile phase	2.3	2.50 ± 0.02	0.89	2.49 ± 0.04	1.94
	2.6	2.50 ± 0.03	1.59	2.50 ± 0.03	1.87
	2.9	2.50 ± 0.03	1.25	2.49 ± 0.09	0.04

<sup>a</sup> Mean of three replicates

Analyses in the concentration of CUR and QU in the stability test in the methanolic solution showed that the percent recovery of CUR and QU were, respectively, 94.1 ± 3.6% and 91.2 ± 3.1% under refrigeration (8 °C), and 98.1 ± 3.4% and 86.5 ± 3.6% at room temperature (25 °C), Figure 5.

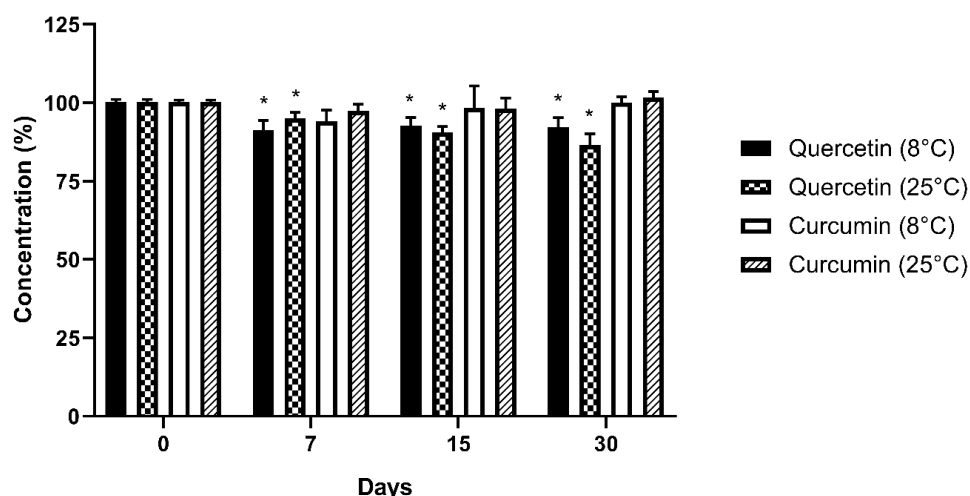


**Figure 5.** Data related to the stability of the standard methanolic solutions of CUR and QU (2.5 µg/mL) at 8°C and 25°C. N=3. \*p < 0.05.

The evaluation of the stability of the free CUR and QU and the nanoencapsulated compounds up to 4 hours in 90:10 PBS:PEG 400, v/v; pH 7.4, at 37°C the percentage of the free form of CUR was  $46.10 \pm 9.4\%$  within 4 hours of evaluation and no QU was detected after 3 hours of experiment. Conversely, the results of the nanoencapsulated compounds showed that after 4 hours of experiment at 37°C the percentage of the CUR and QU were found to be higher, respectively  $69.33 \pm 1.0\%$  and  $5.80 \pm 0.5\%$  (Figure 6).

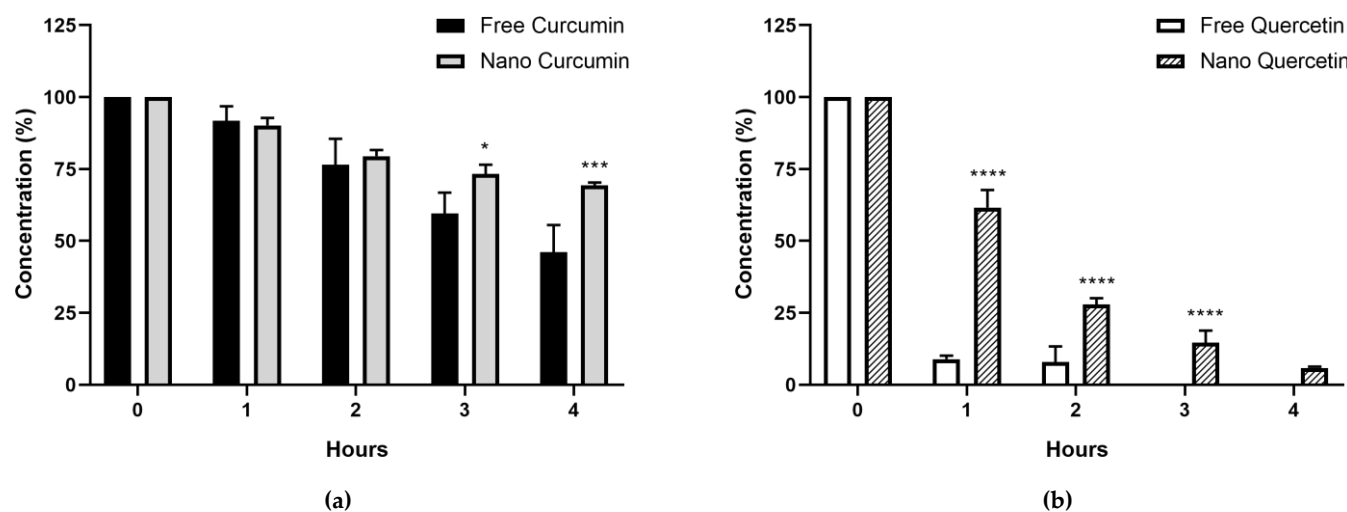


**Figure 6.** Data related to the stability of the free and nanoencapsulated CUR (a) and QU (b) in PBS:PEG400 (90:10) pH 7.4. N=3 at temperature (37°C). \*p < 0.05, \*\*\*p < 0.001, \*\*\*\*p < 0.0001.

### 3.3. Size, polydispersity index, and zeta potential

The formulations containing CUR and QU showed a size of  $119.43 \pm 0.83$  nm, PDI of  $0.202 \pm 0.02$  nm and zeta potential of  $-22.3 \pm 0.15$  mV, and the control nanoemulsion prepared without the active compounds showed a size of  $102.86 \pm 1.80$  nm, PDI of  $0.183 \pm 0.02$  nm and zeta potential of  $-25.7 \pm 0.46$  mV.

### 3.4. Determination of the concentration of curcumin and quercetin in nanoemulsion using HPLC analyses

The formulations containing CUR and QU showed an amount of  $0.71 \pm 0.08$  mg/mL of QU, and  $0.62 \pm 0.08$  mg/mL of CUR, and demonstrated that it was possible to encapsulate  $94.66 \pm 10.6\%$  of QU in the developed nanocarriers and  $82.66 \pm 10.6\%$  of CUR with an entrapment efficiency of  $> 99\%$  for both compounds.

### 3.5. Transmission electron microscopy

The TEM micrographs performed by negative stain illustrated the morphology and size of the nanoemulsion produced (Figure 7). The nanocarriers appeared spherical in shape with size and particle size distribution in good accordance with the results of the analyses performed by dynamic light scattering. Moreover, the nanocarriers were well dispersed without significant agglomeration or morphological variations.

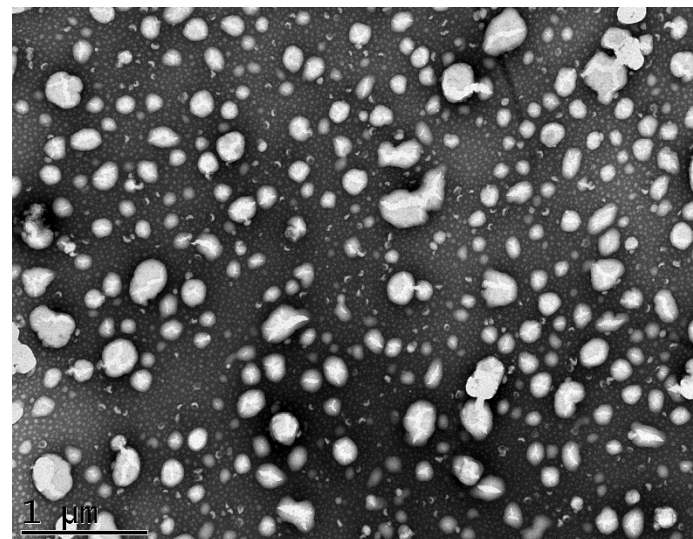


**Figure 7.** Transmission electron micrographs of nanoemulsion with curcumin and quercetin (CQ NE).

#### 4. Discussion

The physicochemical properties of both active ingredients as well of their association were assessed using different techniques such as thermal analyses (TGA and DSC) and powder X-ray diffraction (PXRD).

Initially, the active ingredients and their combination were characterized using thermal analyses, which offer the ability to quickly screen for potential drug–drug incompatibilities. Such interactions can be of physical or chemical nature and may affect the stability and bioavailability of the final product, compromising the therapeutic efficacy and safety [29].

The TGA curve of CUR indicated that the thermal decomposition occurred in two steps, while no water was present in the sample. However, the decomposition for QU was observed in three steps and, contrarily of CUR, the QU presents water molecules into the crystal lattice, influencing in its molecular geometry and crystalline structure, affecting its thermal stability, solubility, and bioavailability. The profile of the binary mixture decomposition was very similar to the pure compounds, meaning that the physical mixture of CUR and QU (1:1 ratio) does not lead to significant interactions in the solid state and the compounds undergo thermal degradation simultaneously and independently.

The DSC technique was employed to analyze the occurrence of physicochemical events related to the thermal behavior and possible interactions between the compounds [30]. It is noteworthy that although such analyses were conducted upon heating the sample to high temperatures, which is not consistent with the process of nanoemulsion production, neither with its administration to patients, they afford important information regarding the physical properties of the samples [29]. The endothermic peak observed in the QU DSC curve can be attributed to the moisture of this compound and is in agreement with the TGA result as soon as the melting point of QU occurs at 316 °C. However, the endothermic peak observed in the CUR DSC curve correspond to the melting point of CUR, and the shoulder that is observed in the DSC curve from 200 °C in the CUR curve correspond to the beginning of the decomposition of this compound, as seen in the TGA curve.

The PXRD analyses of the binary mixture contained virtually all the peaks of CUR and QU, with no marked displacement of the peaks, and no appearance of any new peaks was observed, which means that if exist some interaction between the compounds, this one is probably not strong enough to take place in the solid state.

Considering the unique properties showed by nanoemulsion, in the present work, CUR and QU, castor oil and DHA, as well as egg lecithin composed the oil phase and Milli Q water and PEG stearate composed the aqueous phase. In this context, HPLC-UV was selected as an analytical tool

for the simultaneous quantification of CUR and QU in the developed nanoemulsion through a rapid, simple, and gradient method. The method was validated in accordance with ICH Q2 R1 (validation of Analytical Procedures: Text and Methodology) and CDER-FDA guideline (validation of chromatographic methods). Analytes retention factor, asymmetry and number of theoretical plates ( $N > 2000$ ) were investigated. All obtained values were in accordance with required criteria, indicating the suitability of the analytical method. No other co-eluting peak along with those of interest, the method being specific for the estimation of CUR and QU. The alterations in the conditions of the chromatographic method to evaluate the robustness like, the temperature change, mobile phase composition and pH did not promote any significant variations in the retention time of CUR and QU peaks indicating that the method was robust. The developed and validated method demonstrated to efficiently determine CUR and QU loaded on nanoemulsion vectors. The extraction method of the drug proved to be efficient, since the recovery range of the compounds from the nanoemulsion was between 99.46 and 101.63%.

The preparation method via high-energy emulsification followed by high-pressure homogenization was efficient to obtain the nanoemulsions. The zeta potential that is an important parameter to determine the stability of the formulations, since values higher than 130 mV are considered ideal in terms of electrostatic stability. However, systems that have steric stabilizers such as PEG stearate do not follow this rule, being more stable with wider values of surface charge. Zeta potential values lower than 130 mV, do not represent low stability for the system since a steric stability can be hypothesized [31]. The negative charge observed for the nanoemulsion developed (from -22 to -25 mV) resulted from the presence of charged phospholipids such as phosphatidylserine, phosphatidylinositol, and phosphatidic acid in the lecithin phospholipids mixture [32]. The developed formulations showed an incorporation of high amounts of CUR (0.62 mg/mL) and QU (0.71 mg/mL) in the formulation. The morphological analysis of the nanoemulsions carried with TEM showed that the developed nanocarrier appeared spherical in shape with the size and polydispersity index in good accordance with the results of the analyses performed by dynamic light scattering.

The evaluation of the concentration of CUR and QU during 30 days showed no changes in the amount of the CUR in methanolic solution at 8°C and 25°C, however the One-way ANOVA detected statistically significant differences among the concentration of QU after 7 days at 8°C and 25°C compared to the initial amount of QU. The drugs in methanolic solution were stable for at least 15 days under storage conditions, with RSDs below 8%. The evaluation of the free CUR and QU at the phosphate buffer (90:10, PBS:PEG 400, v/v; pH 7.4) at 25°C showed a higher degradation of QU compared to CUR. However the comparison between the free from of the CUR and QU at the phosphate buffer (90:10, PBS:PEG 400, v/v; pH 7.4) at 37°C showed that the developed nanoemulsion protected at least partially the CUR and QU from the degradation.

## 5. Conclusions

The combination of CUR and QU in a pharmaceutical formulation is of great importance owing to the potential of generating a new option for the treatment of neurodegenerative diseases. In this sense, the study of formulation using different techniques such as TGA, DSC, and PXRD was essential to examine the existence of possible interactions between these two compounds (CUR and QU). Furthermore, an HPLC method was developed and validated according to standard guidelines, and it is the first reported method for the simultaneous determination of CUR and QU in a nanocarrier such as nanoemulsion. The possible interactions between CUR and QU demonstrated no strong enough interaction in the solid-state, and the thermal analysis demonstrated that CUR and QU are stable under the temperatures of the nanoemulsion production. The proposed method was selective and linear in the range of 0.5 – 12.5 µg/mL, precise, robust and accurate with no interfering peaks among the regions of interest. Low detection and quantification limits for CUR and QU obtained were suitable for the application of the method for the studies of drug entrapment efficiency and formulation stability with the developed nanoemulsion. Moreover, it was found that the CUR and QU were better stable into nanoemulsions in the simulated biological fluids, compared to the free material, which could favor a higher bioavailability and consequently drug effectiveness.

**Author Contributions:** Conceptualization, Gustavo Vaz and Adryana Clementino; methodology, Adryana Clementino and Juliana Bidone; validation, Gustavo Vaz, Mariana Falkembach, Matheus Batista and Paula Barros; data curation, Cristiana Dora, Fabio Sonvico, Gustavo Vaz, Marcos Villetti; writing,—original draft preparation, Gustavo Vaz; writing—review and editing, Cristiana Dora and Fabio Sonvico; supervision, Cristiana Dora and Fabio Sonvico; funding acquisition, Cristiana Dora. All authors have read and agreed to the published version of the manuscript.

**Funding:** This study was financed in part by the Coordenação de Aperfeiçoamento de Pessoal de Nível Superior - Brasil (CAPES) Finance Code 001. Grant number 88881.189309/2018-01.

**Acknowledgments:** The authors thank CNPq (Brazilian Council of Research and Development), and the University of Rio Grande (FURG) for the scholarship of the undergraduate students, and the Integrated Analysis Center of the Federal University of Rio Grande, and south electron microscopy center by the analyzes performed. The fellowship from CAPES/Print (Processo 88881.310412/2018-01) is also acknowledged.

**Conflicts of Interest:** The authors declare no conflict of interest.

## References

1. Manach, C.; Scalbert, A.; Morand, C.; Rémesy, C.; Jiménez, L. Polyphenols: food sources and bioavailability. *The Am. J. Clin. Nutr.* **2004**, *79*, 727–747, doi:10.1093/ajcn/79.5.727.
2. Cheong, E. Synthetic and naturally occurring COX-2 inhibitors suppress proliferation in a human oesophageal adenocarcinoma cell line (OE33) by inducing apoptosis and cell cycle arrest. *Carcinogenesis* **2004**, *25*, 1945–1952, doi:10.1093/carcin/bgh184.
3. Mehta, V.; Parashar, A.; Udayabhanu, M. Quercetin prevents chronic unpredictable stress induced behavioral dysfunction in mice by alleviating hippocampal oxidative and inflammatory stress. *Physiol. Behav.* **2017**, *171*, 69–78, doi:10.1016/j.physbeh.2017.01.006.
4. Testa, G.; Gamba, P.; Badilli, U.; Gargiulo, S.; Maina, M.; Guina, T.; Calfapietra, S.; Biasi, F.; Cavalli, R.; Poli, G.; et al. Loading into Nanoparticles Improves Quercetin’s Efficacy in Preventing Neuroinflammation Induced by Oxysterols. *PLoS ONE* **2014**, *9*, e96795, doi:10.1371/journal.pone.0096795.
5. Guo, Y.; Bruno, R.S. Endogenous and exogenous mediators of quercetin bioavailability. *J. Nutr. Biochem.* **2015**, *26*, 201–210, doi:10.1016/j.jnutbio.2014.10.008.
6. Ravichandran, R. Studies on Dissolution Behaviour of Nanoparticulate Curcumin Formulation. *Adv. Nanoparticles* **2013**, *02*, 51–59, doi:10.4236/anp.2013.21010.
7. Sarker, M.R.; Franks, S.F. Efficacy of curcumin for age-associated cognitive decline: a narrative review of preclinical and clinical studies. *GeroScience* **2018**, *40*, 73–95, doi:10.1007/s11357-018-0017-z.
8. Motaghinejad, M.; Motevalian, M.; Fatima, S.; Faraji, F.; Mozaffari, S. The Neuroprotective Effect of Curcumin Against Nicotine-Induced Neurotoxicity is Mediated by CREB–BDNF Signaling Pathway. *Neurochem. Res.* **2017**, *42*, 2921–2932, doi:10.1007/s11064-017-2323-8.
9. Tsai, Y.-M.; Chien, C.-F.; Lin, L.-C.; Tsai, T.-H. Curcumin and its nano-formulation: The kinetics of tissue distribution and blood–brain barrier penetration. *Int. J. Pharm.* **2011**, *416*, 331–338, doi:10.1016/j.ijpharm.2011.06.030.
10. Anand, P.; Kunnumakkara, A.B.; Newman, R.A.; Aggarwal, B.B. Bioavailability of Curcumin: Problems and Promises. *Mol. Pharm.* **2007**, *4*, 807–818, doi:10.1021/mp700113r.
11. Cenini, G.; Lloret, A.; Casella, R. Oxidative Stress in Neurodegenerative Diseases: From a Mitochondrial Point of View. *Oxidative Med. Cell. Longevity* **2019**, *2019*, 1–18, doi:10.1155/2019/2105607.
12. Garaschuk, O. Imaging microcircuit function in healthy and diseased brain. *Exp. Neurol.* **2013**, *242*, 41–49, doi:10.1016/j.expneurol.2012.02.009.
13. Verdile, G.; Fuller, S.J.; Martins, R.N. The role of type 2 diabetes in neurodegeneration. *Neurobiol. Dis.* **2015**, *84*, 22–38, doi:10.1016/j.nbd.2015.04.008.
14. Gupta, R.; Xie, H. Nanoparticles in Daily Life: Applications, Toxicity and Regulations. *J. Environ. Pathol. Toxicol. Oncol.* **2018**, *37*, 209–230, doi:10.1615/JEnvironPatholToxicolOncol.2018026009.
15. Rizvi, S.A.A.; Saleh, A.M. Applications of nanoparticle systems in drug delivery technology. *Saudi Pharm. J.* **2018**, *26*, 64–70, doi:10.1016/j.jps.2017.10.012.
16. Bonferoni, M.; Rossi, S.; Sandri, G.; Ferrari, F.; Gavini, E.; Rassu, G.; Giunchedi, P. Nanoemulsions for “Nose-to-Brain” Drug Delivery. *Pharmaceutics* **2019**, *11*, 84, doi:10.3390/pharmaceutics11020084.
17. Solans, C.; Solé, I. Nano-emulsions: Formation by low-energy methods. *Curr. Opin. Coll. Interface Sci.* **2012**, *17*, 246–254, doi:10.1016/j.cocis.2012.07.003.
18. Thakur, N.; Garg, G.; Sharma, P.K.; Kumar, N. Nanoemulsions: A Review on Various Pharmaceutical Application. *Global J. Pharmacol.* **2012**, *6*, 222–225, doi:10.5829/idosi.gjp.2012.6.3.65135.

19. Comfort, C.; Garrastazu, G.; Pozzoli, M.; Sonvico, F. Opportunities and Challenges for the Nasal Administration of Nanoemulsions. *Curr. Top. Med. Chem.* **2015**, *15*, 356–368, doi:10.2174/1568026615666150108144655.
20. Fornaguera, C.; Solans, C. Analytical Methods to Characterize and Purify Polymeric Nanoparticles. *International J. Polym. Sci.* **2018**, *2018*, 1–10, doi:10.1155/2018/6387826.
21. ICH Topic Q2 (R1) Validation of Analytical Procedures : Text and Methodology, Int. Conf. Harmon. 1995.
22. U. Center for Drug Evaluation and Research, US Food and Drug Administration, Reviewer Guidance, Validation of Chromatographic Methods 1994.
23. Borghetti, G.S.; Costa, I.M.; Petrovick, P.R.; Pereira, V.P.; Bassani, V.L. Characterization of different samples of quercetin in solid-state: indication of polymorphism occurrence. *Pharmazie*. *Pharmazie* **2006**, *61*, 802–804.
24. Borghetti, G.S.; Carini, J.P.; Honorato, S.B.; Ayala, A.P.; Moreira, J.C.F.; Bassani, V.L. Physicochemical properties and thermal stability of quercetin hydrates in the solid state. *Thermochim. Acta* **2012**, *539*, 109–114, doi:10.1016/j.tca.2012.04.015.
25. Olejniczak, S.; Potrzebowski, M.J. Solid state NMR studies and density functional theory (DFT) calculations of conformers of quercetin. Electronic supplementary information (ESI) available: TGA profiles for samples 1 and 2 and <sup>13</sup>C NMR shielding parameters. See <http://www.rsc.org/suppdata/ob/b4/b406861k/>. *Org. Biomol. Chem.* **2004**, *2*, 2315, doi:10.1039/b406861k.
26. Kiran, G.; Kulkarni, A.P. Design, Synthesis and Evaluation of Quercetin-Meclofenamic acid Conjugate: A Mutual Pro-drug for Safer NSAIDs. *Asian J. Med. Pharm. Res.* **2013**, *3*, 18–23.
27. Sayyar, Z.; Jafarizadeh-Malmiri, H. Temperature Effects on Thermodynamic Parameters and Solubility of Curcumin O/W Nanodispersions Using Different Thermodynamic Models. *Int. J. Food Eng.* **2019**, *15*, doi:10.1515/ijfe-2018-0311.
28. Long, Y.; Zhang, W.; Wang, F.; Chen, Z. Simultaneous determination of three curcuminoids in Curcuma longa L. by high performance liquid chromatography coupled with electrochemical detection. *J. Pharm. Anal.* **2014**, *4*, 325–330, doi:10.1016/j.jpha.2013.10.002.
29. Baharate, S.S.; Bharate, S.B.; Bajaj, A.N. Interactions and incompatibilities of pharmaceutical excipients with active pharmaceutical ingredients: A comprehensive review. *J. Excipients Food Chem.* **2010**, *1*, 3–26, doi:10.1016/j.indcrop.2015.11.088.
30. Ceschel, G.C.; Badiello, R.; Ronchi, C.; Maffei, P. Degradation of components in drug formulations: a comparison between HPLC and DSC methods. *J. Pharm. Biomed. Anal.* **2003**, *32*, 1067–1072, doi:10.1016/S0731-7085(03)00210-3.
31. Heurtault, B.; Saulnier, P.; Pech, B.; Proust, J.; Benoit, J. A novel phase inversion-based process for the preparation of lipid nanocarriers. *Pharm. Res.* **2002**, *19*, 875–880, doi:10.1023/A:1016121319668.
32. Dora, C.L.; Silva, L.F.C.; Putaux, J.-L.; Nishiyama, Y.; Pignot-Paintrand, I.; Borsali, R.; Lemos-Senna, E. Poly(ethylene glycol) Hydroxystearate-Based Nanosized Emulsions: Effect of Surfactant Concentration on Their Formation and Ability to Solubilize Quercetin. *J. Biomed. Nanotechnol.* **2012**, *8*, 202–210, doi:10.1166/jbn.2012.1380.